Chemistry and Properties of Cross-Linked All-Aromatic Hyperbranched Polyaryletherketones

Vogel, Wouter; Hegde, Maruti; Keith, Andrew N.; Sheiko, Sergei S.; Dingemans, Theo J.

DOI
10.1021/acs.macromol.1c01998

Publication date
2021

Document Version
Final published version

Published in
Macromolecules

Macromolecules

pubs.acs.org/Macromolecules Article

Chemistry and Properties of Cross-Linked All-Aromatic Hyperbranched Polyaryletherketones

Wouter Vogel, Maruti Hegde, Andrew N. Keith, Sergei S. Sheiko, and Theo J. Dingemans*

Cite This: *Macromolecules* 2022, 55, 100−112 Read Online

ABSTRACT: Thermoplastic polyaryletherketones (PAEKs) exhibit excellent mechanical properties and fluid stability, but their glass transition temperatures (T_g) are low and their all-aromatic nature makes processing challenging. We will present a synthetic route toward phenylethynyl-functionalized hyperbranched PAEKs (*hb*PAEKs) (T_g = 151 °C) that can be cross-linked to form flexible films with high T_g's (187−237 °C) and good mechanical properties (E' = 4 GPa, σ = 44 MPa, and ε = 1.76%). After cross-linking, the films are amorphous, easy to handle, and insoluble. We will report on the melt rheology of the *hb*PAEK precursors, with and without reactive phenylethynyl-reactive functionalities, and the thermomechanical characteristics of thin cross-linked films using dynamic mechanical thermal analysis, differential scanning calorimetry, and tensile testing. We believe that our findings can be extended to other all-aromatic structural and functional polymer architectures that are otherwise impossible to process.

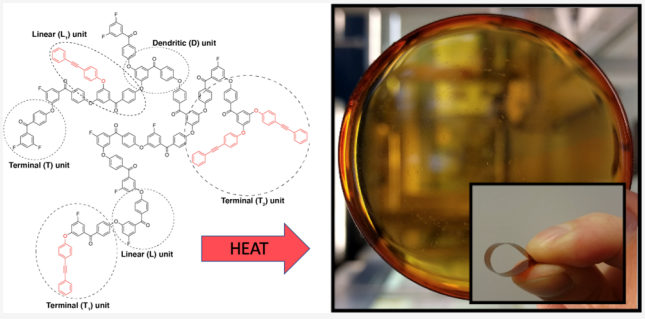

1. INTRODUCTION

Aromatic polyaryletherketones (PAEKs) are a family of high-performance thermoplastic polymers that offer excellent thermomechanical properties and fluid stability. Well-known examples include linear polyetheretherketone (PEEK) (**I**) and polyetherketoneketone (PEKK) (**II**), Scheme 1. Both polymers are semicrystalline and characterized by high melting points (T_m > 340 °C) and relatively low glass transition temperatures (T_g) of 140 and 155 °C, respectively.[1]

When using monomers of the AB_2 or A_2 + B_3 type, all-aromatic hyperbranched (*hb*) PAEKs (*hb*PAEKs) can be obtained that exhibit a branched globular topology.[2] This globular topology yields polymers with physical properties that are markedly different from their linear analogues. For example, the branched structure enhances solubility of *hb* polymers in a wide range of common solvents,[3] and the lack of chain entanglements yields low-viscosity solutions and melts.[4,5] At the same time, a lack of chain entanglement results in rather poor mechanical properties such as low strength and poor ductility, which limits their practical use.[6,7] With respect to the thermal properties, a hyperbranched architecture offers tunability of T_g, which can be varied between 95 and 250 °C for *hb*PAEKs by choice of an appropriate end-group functionality.[8] One of the goals of this study is to explore a synthetic route toward *hb*PAEKs that can be processed from the melt or common solvents into parts with useful mechanical properties and exhibit T_g values >200 °C.

One approach toward preparing mechanically robust *hb*PAEKs is to introduce covalent bonds between adjacent globules using reactive end groups. Propargyl,[9] epoxide,[10] and phthalonitrile end groups[11] have been incorporated in *hb*PAEK imides,[9] polyarylethersulfones,[10] and PAEKs,[11] respectively. The choice of the cross-linkable end group will affect the physical properties of the *hb* polymer, considering that T_g is strongly dependent on end-group polarity.[12] Additionally, the type of end group can affect the thermal stability of the final cross-linked aromatic *hb* polymer—cross-linkable aliphatic end groups can be expected to result in a reduction in thermal stability. However, such thermal stability issues can be mitigated by the use of thermally cross-linkable end groups based on (phenyl)alkynes, which are known to produce aromatic polymers with excellent high-temperature thermomechanical properties.[13−15] Despite the fact that several synthetic strategies toward producing cross-linked *hb* polymeric networks have been published,[9−11,16] the relationship between end-group chemistry, cross-link density, processing, and the final mechanical properties of cross-linked aromatic *hb* polymers is poorly understood.

In this paper, we will present a series of *hb*PAEKs that have been functionalized with different concentrations of 4-(phenylethynyl)phenol (PEP) end groups that can be further reacted in a controlled fashion using a high-temperature

Received: September 22, 2021
Revised: December 7, 2021
Published: December 29, 2021

https://doi.org/10.1021/acs.macromol.1c01998
Macromolecules 2022, 55, 100−112

Scheme 1. Molecular Structures of PEEK and PEKK

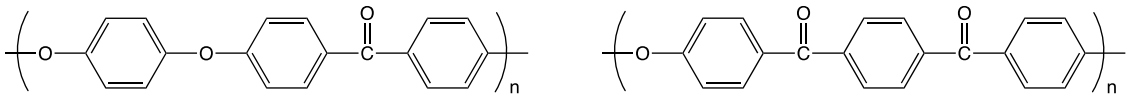

Polyetheretherketone (PEEK) (**I**)
Tg = 140 °C and Tm = 344 °C

Polyetherketoneketone (PEKK) (**II**)
Tg = 155 °C and Tm = 384 °C

treatment step at 350 °C. We will report on melt rheology during cross-linking and show that cross-linking is the result of chemistry between the remaining −F and −OH functionalities present on the *hb*PAEK structure and reactions between phenylethynyl end groups. A comparison of the thermal properties of the *hb*PAEKs, before and after cure, will be presented. Additionally, we will demonstrate that it is possible to prepare flexible cross-linked *hb*PAEK films with high T_g's that are handleable and exhibit good stress−strain behavior.

2. EXPERIMENTAL SECTION

2.1. Materials. 3,5-Difluorobenzoyl chloride was purchased from Alfa Aesar. Dry *N*-methyl-2-pyrolidone (NMP) and dry toluene were obtained from Acros Organics and used as received. 4-Iodophenol was purchased from TCI and $Pd(PPh_3)_2Cl_2$ and PPh_3 were purchased from Sigma-Aldrich and used as received. Phenylethynyl was also purchased from Sigma-Aldrich and vacuum-distilled before use. Triethylamine was purchased from Alfa Aesar. A reference PEKK film sample was obtained from Solvay (Ajedium film CYPEK FC) and used as received.

2.2. Synthetic Details. *2.2.1. 3,5-Difluoro-4′-hydroxybenzophenone, AB_2.* A 1 L round-bottom flask was charged with 50 g (0.2 mol) of (3,5-difluorophenyl)(4-methoxyphenyl)methanone, which was synthesized according to the procedure described in the literature.[8] To the flask was added 450 mL of acetic acid, and the mixture was stirred and heated to 50 °C until a transparent solution was obtained. Then, 300 mL of HBr (48%) was added and a white precipitate was formed. The mixture was heated to 130 °C for a steady reflux (the mixture became transparent at 100 °C). The reaction mixture was stirred overnight, and thin-layer chromatography [dichloromethane (DCM) as an eluent] confirmed the completion of the reaction (1 spot, R_f = 0.2). The reaction mixture was cooled, and the mixture was evaporated to dryness. The white/pinkish solid was added to 1.5 L of water and extracted with 3 × 300 mL of ether. The product was recrystallized from 100% EtOH and dried overnight in vacuum at 60 °C, resulting in 43.1 g of the target compound as a white solid, 91%. mp 150−151 °C. FT-IR (cm^{-1}): 3400−3000, 1640, 1582, 1438, 1329. MS (EI) *m*/*z*: 234 (M), 121. ^{1}H NMR (DMSO-d_6): δ 10.58 (s, 1H), 7.9 (d, *J* = 8.7, 2H), 7.51−7.47 (tt, *J* = 2.4 Hz, 1H), 7.31−7.29 (m, 2H), 6.90 (d, *J* = 8.7, 2H). ^{13}C NMR (DMSO-d_6): δ 191.98, 163.67, 163.06, 161.20, 142.01, 133.12, 127.20, 115.89, 112.54, 107.34. Elemental Anal. Calcd for $C_{13}H_8F_2O_2$: C, 66.67; H, 3.44; F, 16.22. Found: C, 66.58; H, 3.37; F, 16.06.

2.2.2. Fluorine-Terminated hbPAEK with 9.2k g/mol Molecular Weight. To a 250 mL round-bottom flask equipped with Dean−Stark trap were added 15 g of AB_2 monomer, 100 mL of dry NMP, 75 mL of dry toluene, and 15 g of K_2CO_3. This was stirred for 3 h at 165 °C, while the toluene/water azeotrope was collected. The temperature was subsequently increased over 30 min to 200 °C for a period of 180 min. The mixture was cooled to r.t. and precipitated in 3 L of water. The collected solid was dissolved in tetrahydrofuran (THF) and precipitated in MeOH, and the collected solid was boiled in MeOH, filtered hot, boiled in EtOH, filtered hot, and dried in vacuo at 60 and 150 °C overnight to obtain the target compound as off-white and very fine powder, 11.2 g, 82%. FT-IR (cm^{-1}): 1663, 1581, 1501, 1435, 1321, 1233. ^{1}H NMR (400 MHz, $CDCl_3$): δ 7.90−7.50 (m, 2H), 7.30−6.50 (m, 5H). Specific molecular weights (MWs) can be targeted by varying the reaction time at 200 °C.

2.2.3. 4-(Phenylethynyl)phenol. We synthesized PEP using a previously reported procedure with a slightly modified work-up procedure.[17] To a clean, dry, 1 L one-neck round-bottom flask were added $Pd(PPh_3)Cl_2$ (0.8 g, 1 mmol), CuI (0.43 g, 2 mmol), and PPh_3 (0.30 g, 1 mmol). The flask was placed under vacuum and subsequently backfilled with argon. 4-Iodophenol (25 g, 0.11 mmol) in 650 mL of Et_3N and phenylacetylene (16.35 mL, 0.15 mol) in 150 mL of Et_3N were added. This was stirred for 24 h before the yellow suspension was filtered, washed with Et_3N, and concentrated. The resulting dark oil was purified via column chromatography over silica in DCM (R_f = 0.2) to give the desired product PEP as a slightly orange product (19 g, 87%). MS (EI), *m*/*z*: 194 (M). FT-IR (cm^{-1}): 3400−3000, 2225, 1608, 1590, 1509, 1440, 1371. MP: 125 °C. ^{1}H NMR ($CDCl_3$): δ 7.53−7.51 (d, 2H), 7.44−7.42 (d, 2H), 7.34−7.33 (d, 3H), 6.82−6.80 (d, 2H), 5.2−4.6 (b, 1H). ^{13}C NMR ($CDCl_3$): 155.57, 133.27, 131.44, 128.31, 127.99, 123.48, 115.67, 115.50, 89.20 (acetylene), 88.09 (acetylene).

2.2.4. Synthesis Example of PEP-Terminated hbPAEK: hbPAEK-9.4k−25 mol % PEP. To a 100 mL flask was added 2 g of neat *hb*PAEK-9.4k (8.54 mmol) and this was dissolved in 30 mL of NMP. K_2CO_3 (0.47 g, 3.4 mmol) and PEP (0.33 g, 1.7 mmol) were added and the solution was stirred at 140 °C for 4 h. No Dean−Stark trap was used. The dark solution was precipitated in ice-cold water and neutralized with 1 M HCl. The precipitate was collected, dried in vacuo at 60 °C overnight, dissolved in THF, and precipitated in methanol. The pale yellow/white solid was dried in vacuo at 60 °C for 24 h. The yield was quantitative. ^{1}H NMR (400 MHz, $CDCl_3$): δ 7.90−7.50 (m, 2H), 7.30−6.50 (m, 5H). ^{13}C NMR ($CDCl_3$): 192.88, 162.89, 160.30, 140.72, 132.61, 118.88, 116.48, 112.78, 107.70, 94.47 (acetylene), 89.03 (acetylene).

2.3. Characterization. Differential scanning calorimetry (DSC) experiments were performed using a TA Instruments 2500 series at 10 or 20 °C/min under a nitrogen atmosphere in crimped aluminum sample pans. All curves reported are obtained during the first heating. Thermogravimetric analysis (TGA) measurements were performed on a TA instruments 5500 TGA at 10 °C/min under nitrogen purge in aluminum pans. ^{1}H NMR (400 MHz) and ^{13}C-NMR (100 Hz) spectra were recorded on a Varian AS-400 spectrometer, and chemical shifts are given in ppm (δ) relative to tetramethylsilane as an internal standard. The ^{1}H NMR splitting patterns are designated as follows: s (singlet), d (doublet), dd (double doublet), t (triplet), q (quartet), m (multiplet), and b (broad signal). The coupling constants, if given, are reported in Hertz. Size-exclusion chromatography (SEC) measurements were performed using a Shimadzu GPU DHU-20A3 equipped with an LC-20AD pump (flow rate 0.5 mL/min), two Shodex LF-804 columns in parallel operating at 60 °C, and a refractive index detector; polystyrene standards were used for calibration of the instrument. All samples were dissolved at a 1 mg/mL concentration in NMP and filtered over a 0.45 μm PTFE filter prior to use. Samples for mass spectrometry were analyzed on a Shimadzu GC/MS-QP2010S in the electron-impact ionization (EI) mode, equipped with a direct introduction probe with a heating controller operating at 20 °C/min. Data were acquired and processed using GCMS solution software. FT-IR spectra were recorded using powdered samples on a PerkinElmer spectrum 100 FT-IR spectrometer, measured from 600 to 4000 cm^{-1}. Isochronal, parallel-plate oscillatory rheology measurements were performed on polymer powders with a TA Instruments ARES G2, 8 mm parallel plates, 1 Hz, 2% strain, N_2 atmosphere. A heating rate of 5 and 10 °C/min was employed for *hb*PAEK and *hb*PAEK−PEP, respectively. Both samples were subjected to a 1 h

https://doi.org/10.1021/acs.macromol.1c01998
Macromolecules 2022, 55, 100−112

Scheme 2. Synthetic Route Used to Prepare *hb*PAEK−PEP; the Molecular Structure of *hb*PAEK-PEP Is Expanded to Show Dendritic (D), Linear (L), and All Terminal (T) Monomeric Units; and the PEP-Containing Linear and Terminal Units Are Marked as L_1, T_1, or T_2, where the Subscripts Indicate the Number of PEP Groups Attached

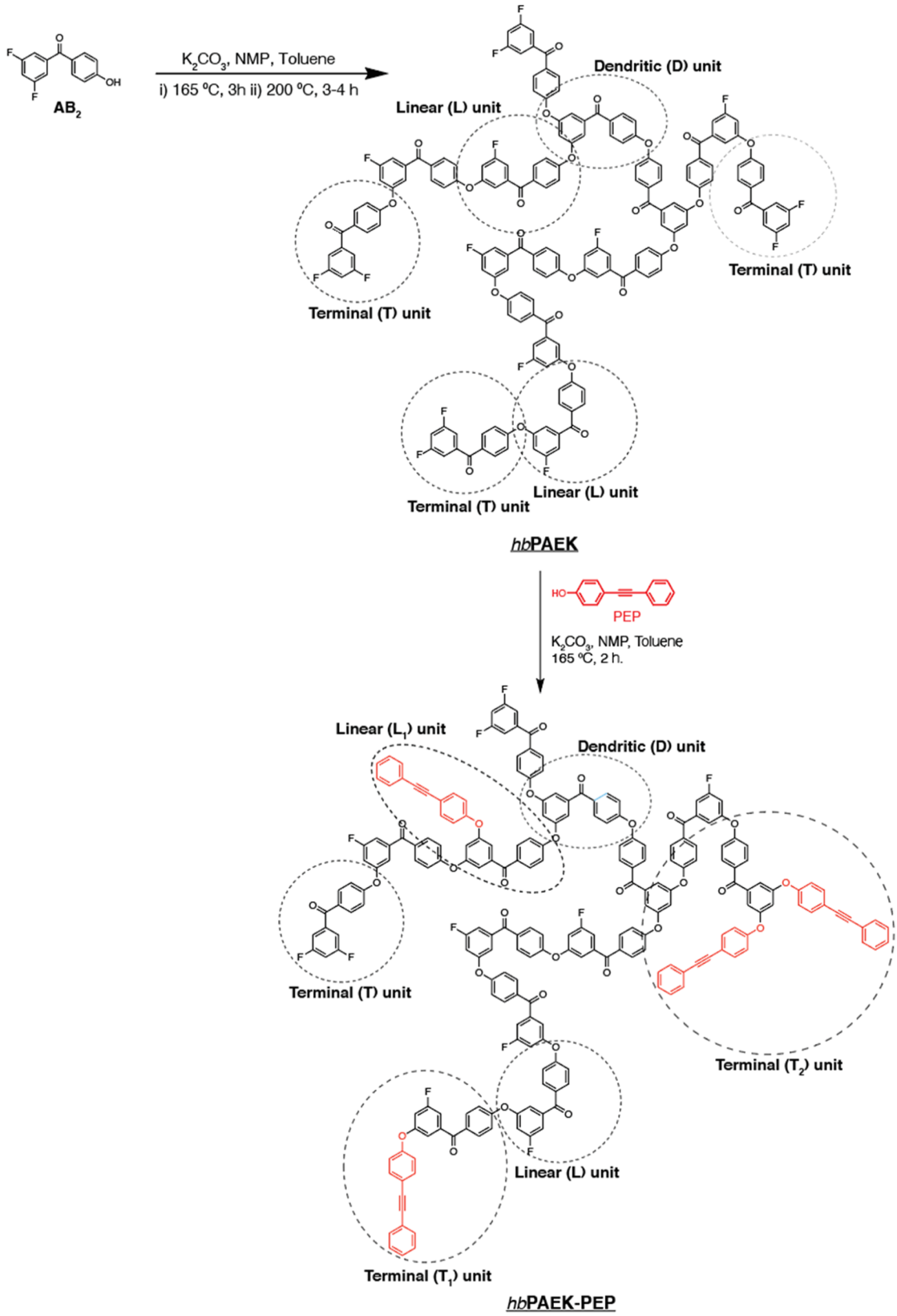

isothermal hold at 350 °C. The isochronal stress-relaxation experiments and curing with PEP were performed on a Thermo Scientific Haake Mars III, 8 mm parallel plates, 1 Hz frequency with 2% strain. Dynamic mechanical thermal analysis (DMTA) was performed on

https://doi.org/10.1021/acs.macromol.1c01998
Macromolecules 2022, 55, 100−112

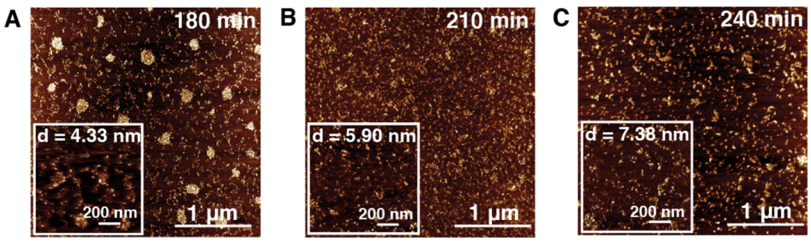

Figure 1. AFM height micrographs of the *hb*PAEKs polymerized for (A) 180, (B) 210, and (C) 240 min. Samples were prepared by spin-coating dilute *hb*PAEK solutions (30 μg/mL in $CHCl_3$) on mica substrates, and individual *hb*PAEK globular diameters (d) are lateral dimensions of individual globules measured using Nanoscope analysis software (section tool) from Bruker. The insets are magnified images (scale bar = 200 nm) of a central area in the main image to help visualize the *hb* globules. Although clustering of *hb*PAEKs is observed in Figure 1A, the magnified images reveal globular particles assigned to individual *hb* macromolecules given their spherical dimensions that progressively increase with monomer conversion. The average globular diameter (d) from lateral dimensions is listed in the inset, and the value $d/2$ is used to calculate the *hb*PAEK's MW.

Table 1. *hb*PAEK Globular Dimensions from AFM, Calculated MW, Relative MWs, and DI from SEC Measurements

*hb*PAEK polymerization time at 200 °C (min)	d^a (nm)	R (nm)	MW[b] (g·mol^{-1})	DB[c]	M_n from SEC[d] (g·mol^{-1})	M_w from SEC[e] (g·mol^{-1})	DI	N^e
180	4.33	1.68	32,266	0.47	9200	22,000	2.4	42.7
210	5.90	2.30	83,721	0.50	9450	69,000	7.3	43.8
240	7.38	2.86	159,755	0.51	9800	123,000	12.5	45.4

[a]Globular diameters (d) are statistical averages of lateral dimensions of individual *hb*PAEK globules from AFM measurements. [b]MW values are calculated using eq 1. [c]DB was calculated from integration values obtained from the ^{19}F NMR spectrum. [d]M_n and M_w values from SEC measurements are obtained from comparison with linear polystyrene standards. [e]All calculations are based on M_n from SEC and are shown in the Supporting Information.

films (20.0 × 3.0 × 0.05 mm) using 0.1, 1, and 10 Hz, at a heating rate of 2 °C/min, under a nitrogen atmosphere with a PerkinElmer Diamond DMTA. Only the storage modulus (E') and loss modulus (E'') data collected at 1 Hz are reported. Stress−strain experiments were performed on an Instron 3365 equipped with a load cell of 1 kN at a constant strain rate of 0.1 mm/min using cured thin-film samples (30.0 × 3.0 × 0.05 mm). The gauge length was set at 2 cm. The Young's modulus was determined by fitting stress−strain curves below 0.1% strain. Elemental analysis was performed by Mikroanalytisches Laboratorium KOLBE in Germany using ICP with an accuracy of 0.01%. The results are an average of two measurements. Atomic force microscopy (AFM) has been utilized to visualize the hyperbranched architecture of the *hb*PAEK prior to cross-linking. All samples were deposited by spin-casting on a mica substrate from chloroform (30 μg/mL). Imaging was performed in the peak-force quantitative nanomechanical property mapping mode using a multimode atomic force microscope (Bruker) with a NanoScope V controller and silicon probes (resonance frequency of 70 Hz and spring constant of 0.4 N/m). Film-casting was performed from NMP (10 w/w % solution) in a Petri dish (6 cm diameter). The cast solutions were placed in a vacuum oven and heated stepwise using the following heating protocol: 1 h at 30 °C, 1 h at 45 °C, 1 h at 60 °C, 1 h at 100 °C, 1 h at 200 °C, 1 h at 300 °C, and 1 h at 350 °C. The films were allowed to cool to room temperature overnight.

3. RESULTS AND DISCUSSION

3.1. Synthesis of PEP-Terminated *hb*PAEKs. Using 3,5-difluoro-4′-hydroxybenzophenone, an AB_2 monomer, the *hb*PAEK is generated through the nucleophilic displacement of the activated fluoro groups by the nucleophilic phenolate ions in NMP, a polar, aprotic solvent (Scheme 2).[18] Despite the *meta*-position of the benzoyl group, an electron-withdrawing group, the fluoro groups in the AB_2 monomer are sufficiently activated to undergo nucleophilic aromatic substitution reactions.[19] The phenolate ions that serve as nucleophiles are generated by the acid−base reaction between phenolic groups on the AB_2 monomer and the base, in this case anhydrous potassium carbonate.[18] A Dean−Stark trap enables azeotropic removal of water formed during the polymerization reaction. The polymerization reaction time determines the final *hb*PAEK MW—*hb*PAEKs were polymerized for 180, 210, and 240 min in this work. In the absence of side reactions, the synthesized *hb*PAEK is expected to be of the form AB_n or B_n (in Scheme 2, the B_n type of *hb*PAEK is shown), where n is related to the degree of polymerization (N) by $n \approx N + 1$. All *hb*PAEKs are obtained by precipitation and are purified using a series of washing steps employing successive dissolution followed by precipitation in hot methanol. The obtained *hb*PAEKs were characterized using ^{1}H NMR (Figure S1, Supporting Information) and ^{13}C NMR spectroscopic techniques.

The synthetic procedure used to prepare *hb*PAEK-PEP, the PEP-functionalized analogue of *hb*PAEK, is shown in Scheme 2.

Through a post-polymerization nucleophilic aromatic substitution reaction, the fluoro atoms on the *hb*PAEK can be displaced with PEP, yielding the reactive *hb*PAEK−PEP (Scheme 2). The PEP-reactive end group in turn is synthesized via a Sonogoshira coupling reaction using 4-iodophenol and phenylethynyl. The presence of acetylenic groups in the *hb*PAEK−PEP was confirmed using ^{13}C NMR (see the Experimental Section) and Raman spectroscopy (Figure S2, Supporting Information).

3.2. *hb*PAEK MW and Architecture. Three different MWs of *hb*PAEKs were obtained by polymerizing the AB_2 monomer for 180, 210, and 240 min, respectively. AFM is an effective technique for imaging and dimensional characterization of individual macromolecules.[20−23] Figure 1 shows AFM micrographs of the *hb*PAEKs on a mica substrate and confirms their globular structure.

The measured cross sections of the dense hyperbranched core yield the representative radius ($R = d/2$) of the three-dimensional (3D) spherical globule (Figure S3, Supporting

https://doi.org/10.1021/acs.macromol.1c01998
Macromolecules 2022, 55, 100−112

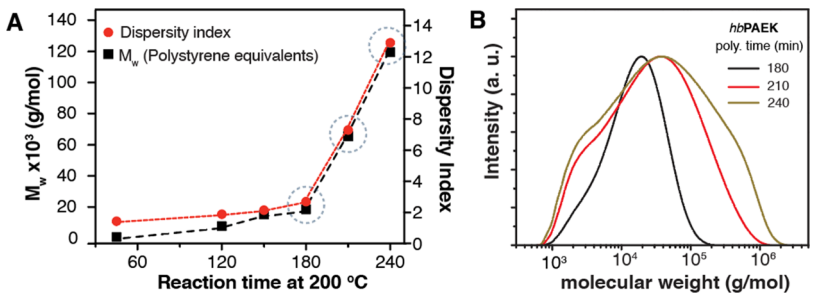

Figure 2. MW and DI from SEC measurements. (A) PS equivalent M_w and DI as a function of reaction time at 200 °C. The circled data points correspond to the *hb*PAEK polymers that were measured using AFM. (B) MW distribution for the three circled data points, that is, at 180, 210, and 240 min, in (A) broadens with increasing reaction time at 200 °C.

Table 2. Characterization of Fluoro and Hydroxy Groups Present in the *hb*PAEKs after Work-Up

*hb*PAEK M_n (g/mol)	theoretical[a] (% F)	measured[b] (% F)	theoretical no. of fluoro groups[a]	calculated no. of fluoro groups[a]	calculated no. of hydroxyl groups[a]
9200	8.80	6.82	43	33	10
9450	8.80	6.91	44	35	9
9800	8.81	7.78	45	40	5

[a]Calculations are shown in the Supporting Information. [b]Ion chromatography elemental analysis.

Information) and increase with polymerization time (see Figure 1, and Table 1). Using the measured average radius, the molecular volume (V) of individual *hb* globules can be estimated, assuming a spherical shape, which in turn enables an estimation of the MW using eq 1.

$$\mathrm{MW} = N_A \cdot \rho \cdot V \tag{1}$$

where N_A is the Avogadro number, ρ is taken as the density of linear, amorphous PEEK, and $V = (4/3)\pi R^3$.

Using the measured R values (Table 1) in eq 1 yields MW values of 32,266, 83,721, and 159,755 g·mol^{-1} for polymerization times of 180, 210, and 240 min, respectively. We do note that these values are estimates since AFM measurements are affected by the shape and size of the AFM tip.[20] Additionally, the assumption that the *hb*PAEK globules are perfectly dense, spherical structures will also impact MW calculations.[20]

We utilized SEC to track MW as a function of reaction time at 200 °C and the results are summarized in Table 1 and in Figure 2.

SEC measurements provide relative MWs as the peaks are integrated against linear polystyrene calibration standards, a method that is in line with other papers, where *hb*PAEK MWs are reported.[8,24] The polystyrene equivalent weight-average molecular weight (M_w) increases slowly during the first 180 min of the polymerization reaction. After 180 min, *hb*PAEK with an M_w of 22,000 g/mol, an M_n of 9200 g/mol, and a dispersity index (DI) of 2.4 is obtained (Table 1). Polymerization beyond 180 min results in a rapid and linear increase in MW and DI; at 240 min, M_w = 123,000 g/mol, M_n increases marginally to 9800 g/mol, and DI = 12.5 (Table 1). Although the trend in MW as a function of reaction time at 200 °C is consistent with kinetics of step-growth polymerization, the measured DI is much higher than what has been reported for analogous *hb*PAEK polymers.[8,11] The work of Paul Flory demonstrated that statistical polymer growth results in an increase in DI with increasing conversion assuming the consumption of −OH groups during polymerization.[25] However, the dramatic change in DI suggests that hydrolysis side reactions, that is, generation of −OH groups, are primarily responsible for the large DI. The sharp change in DI also indicates that hydrolysis takes place at 200 °C and is prevalent when the polymerization reaction time is extended beyond 180 min. A more detailed investigation of the formed *hb*PAEK architecture as shown below confirms hydrolysis side reactions.

Any *hb*PAEK polymer is comprised of three types of monomeric units: dendritic (D), linear (L), and terminal (T) (see Scheme 2). The respective amounts of these monomeric units in an *hb*PAEK polymer define the branched polymer architecture and can be quantified using a parameter called degree of branching (DB).[8] For our *hb*PAEKs, the DB can be calculated by integration of the L and T fluorine atoms in the ^{19}F NMR spectrum (Figure S4, Supporting Information).[8] Based on work by Hawker and Chu, the number of D units is approximated to be equal to the number of T units.[8] The values thus obtained by integration of the ^{19}F NMR signals can be inserted into the following equation for DB

$$\mathrm{DB} = \frac{2T}{2T + L} \tag{2}$$

All three *hb*PAEK samples, polymerized for 180, 210, and 240 min, have a DB value around 0.5 (Table 1), which is the statistically expected value for these hyperbranched polymers.[26] The theoretical amounts of D, L, and T monomeric units in *hb*PAEK is related to the degree of polymerization (N) by

$$N = T + D + L \tag{3}$$

The MW is in turn related to N by

$$\mathrm{MW} = M_o \times N \tag{4}$$

where M_o is the average MW of the repeat unit.

The average MW for the *hb*PAEK repeat unit (M_o) was calculated to be 215.7 g·mol^{-1} (see detailed calculations in the Supporting Information). Using values for M_n from SEC measurements and M_o in eq 4 yields N = 42.7, 43.8, and 45.4 for polymerization times of 180, 210, and 240 min, respectively (Table 1)—similar calculations for MW obtained using AFM measurements are shown in the Supporting Information. Using N, the resulting monomeric amounts can be calculated and

https://doi.org/10.1021/acs.macromol.1c01998
Macromolecules 2022, 55, 100−112

Scheme 3. Hydrolysis Side Reactions and the Resulting Hydroxy-Functionalized Linear and Terminal Units; (A) Hydrolysis of a Potassium Phenoxide Moiety Forming KOH; (B) New Linear Unit (L′) Formed from the Hydrolysis of a Linear Unit, L; (C) New Terminal Units T′ and T″ Formed after Partial or Complete Hydrolysis of a Terminal Unit T; and (D) New Terminal Unit (T_1′) Formed from Hydrolysis of a Terminal Unit T_1

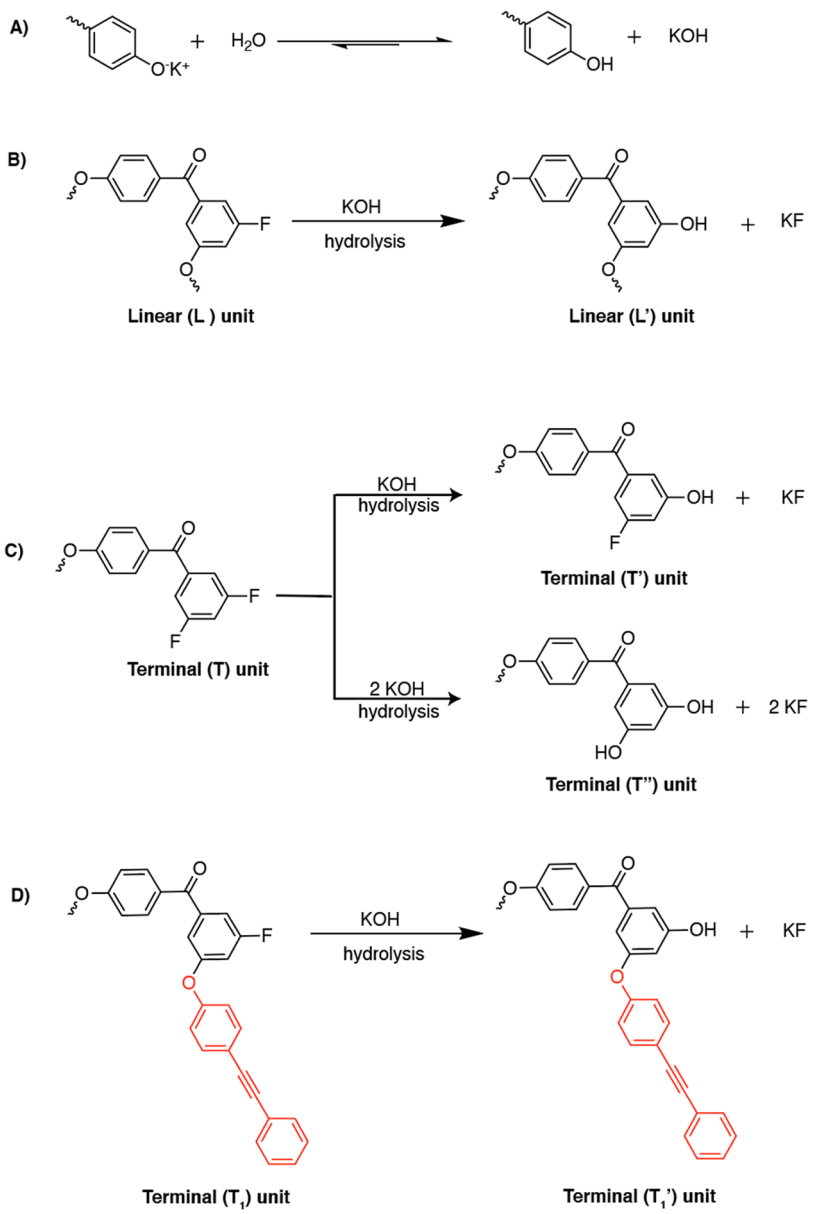

used as input to compute the theoretical wt % of fluorine atoms expected to be present in each *hb*PAEK (Table 2)—calculations are shown in the Supporting Information. The calculated fluorine content in *hb*PAEK is nearly independent of MW, that is, a fluorine content of ∼8.80% is obtained using either MW from AFM measurements (see the Supporting Information) or M_n from SEC measurements. Additionally, ion chromatography (IC) elemental analysis provides an accurate quantification of the fluorine atom amount (weight %) actually present in the *hb*PAEKs (Table 2).[27]

From Table 2, the lack of agreement between the theoretical estimate—using either MW from AFM measurements (see the Supporting Information) or M_n from SEC measurements—and the measured fluorine amount from elemental analysis confirms hydrolysis of some fluoro groups to hydroxyl groups (Scheme 3). The difference between the two can be attributed to the amount of hydroxyl groups present (Table 1) as part of the *hb*PAEK globule. Additionally, the presence of multiple hydroxy groups in *hb*PAEKs also implies that the architecture of the synthesized *hb*PAEK is of the form A_xB_y—where x and y are amounts of hydroxy and fluoro groups listed in Table 2—rather than the expected $AB_{(x+y)}$ or $B_{(x+y)}$ (as shown in Scheme 2). The new linear (L′) unit and three terminal monomeric units, T′, T″, and T_1′ resulting from hydrolysis side reactions are shown in Scheme 3B−D.

The L′ and T″ units (Scheme 3) cannot be directly measured using ^{19}F NMR since they lack fluorine atoms. Additionally, the ^{19}F NMR signal arising from the T′ unit may overlap with that from the L unit (Figure S4, Supporting Information). However, given the minor amount of hydroxy groups in comparison with the total number of fluoro groups present (Table 2), we assume the DB calculation from ^{19}F

https://doi.org/10.1021/acs.macromol.1c01998
Macromolecules 2022, 55, 100−112

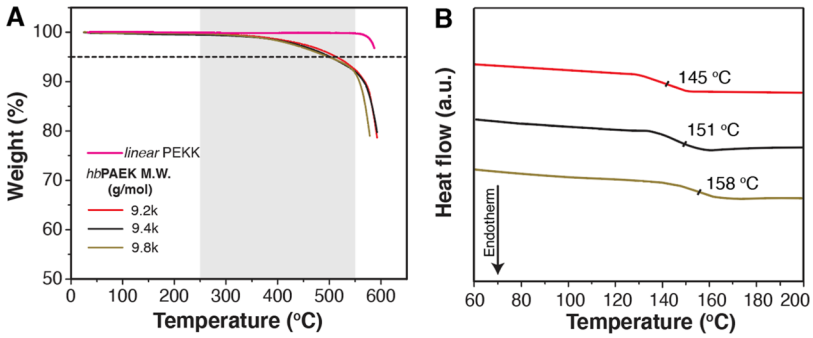

Figure 3. Thermal properties of the *hb*PAEKs prepared at different reaction times at 200 °C. (A) TGA (10 °C/min, N_2 atm) of the *hb*PAEKs. A comparison of TGA curves of *hb*PAEKs with that of commercially available PEKKs shows a significant weight loss between 250 and 550 °C (shaded region) prior to the main degradation event at 550 °C. (B) DSC curves (10 °C/min, N_2 atm, first heat) of the *hb*PAEKs used for this study. All *hb*PAEKs are amorphous and exhibit clear glass transition temperatures (T_g). The legend for both figures is shown in (A).

NMR to still be valid. The new monomeric units, L′, T′, T″, and T_1' from hydrolysis side reactions can continue to polymerize unlike in a linear PAEK, where hydrolytic side reactions will cause a stoichiometric imbalance resulting in oligomeric PAEKs.

Despite the use of anhydrous reagents and polymerization conditions, including the use of a Dean−Stark trap for azeotropic removal of water, our results confirm that water removal during phenolate formation at 165 °C is incomplete or that all hydroxy groups were not converted to phenolates. Once the Dean−Stark trap is removed and the reaction temperature is increased to 200 °C, remnant water or the water now formed due to phenolate formation will result in partial hydrolysis of fluorine groups.[28] Henceforth, the three *hb*PAEK polymers will be identified using the notations *hb*PAEK-9.2k, *hb*PAEK-9.4k, and *hb*PAEK-9.8k, where the MWs denote the MWs (M_n) as obtained from SEC measurements.

3.3. Thermal Behavior of the *hb*PAEKs. Linear PAEKs exhibit high thermal stabilities due to their fully aromatic backbone with temperatures for 5% weight loss ($T_{d,5\%}$) >500 °C, see TGA of a commercially available linear PEKK sample (Figure 3A). However, despite a similar chemical structure, the TGA scans of our *hb*PAEKs at 10 °C/min in a nitrogen atmosphere reveals ∼10 wt % loss (Figure 3A, and Table 3) between 250 and 550 °C, that is, before onset of the main degradation event at 550 °C.

Analysis of the evolved gases using a mass spectrometer reveals HF gas evolution at high temperatures (Figure S5, Supporting Information) and is believed to be the byproduct of a thermal post-condensation reaction between hydroxy and fluoro groups. The post-condensation reaction is also confirmed by SEC measurements. When *hb*PAEK-9.8k was thermally treated at 180, 200, and 240 °C for 1 h each, both M_n and M_w increased by 3.4% (M_n increased to 10,130 g·mol^{-1}) and 19.8% (M_w increased to 147,350 g·mol^{-1}), respectively. Although other authors have reported successful syntheses of *hb* polyamides and *hb* polyesters through melt polycondensation using AB_2 monomers,[29,30] we believe that this is the first instance of thermal post-condensation observed in *hb*PAEKs. We do note that apart from HF, other molecular fragments that could not be identified were also detected during heating of the *hb*PAEKs in the mass spectrometer. We speculate that these molecular fragments are low-MW impurities—dimers and trimers trapped within the *hb* globules that volatilize or thermally degrade between 250 and 550 °C in TGA.

The presence of multiple hydroxy and fluoro groups on the *hb*PAEK globular surface enables the formation of a cross-linked *hb*PAEK network at temperatures above ∼250 °C. Cross-linking of the *hb*PAEKs was confirmed by the formation of insoluble gels during sol−gel testing. The extent of cross-linking is dependent on the temperature used. When the *hb*PAEKs heated between 250 and 300 °C are subjected to sol−gel tests, a small amount of insoluble gel is observed, indicating that the extent of cross-linking achieved is low—accurate quantification of the gel content was not possible due to difficulty in separating the gel from the solution. Significant cross-linking is observed when the *hb*PAEKs are heated above 300 °C. An insoluble gel content of 70−75% is obtained when the *hb*PAEKs are heated between 325 and 350 °C for 1 h, and the gel content increases to 98% when *hb*PAEK is heated at 375 °C for 1 h.

DSC confirms the amorphous nature of the synthesized *hb*PAEKs. The strong dependence of T_g on end-group type (polar vs nonpolar) and the inhibition of segmental motion due to the branched architecture has led to speculation that translational motions are primarily responsible for T_g.[12] The *hb*PAEKs exhibit T_g values that range from 145 to 158 °C, which is in line with what has been published previously,[8] and the T_g values increase with MW (Figure 3B and Table 3). The T_g of the *hb*PAEKs increases upon heat treatment at 350 °C for 1 h by 5−13 °C, which is attributed to cross-linking reactions (Table 3).

Table 3. Thermal Properties of the *hb*PAEKs before and after Cross-Linking at 350 °C as Obtained from TGA and DSC Measurements

*hb*PAEK MW (g/mol)	as-prepared		after cross-linking at 350 °C for 1 h
	$T_{d,5\%}$[a] (°C)	T_g[b] (°C)	T_g[c] (°C)
9200	514	145	158
9450	502	151	156
9800	499	158	169

[a]The temperature for 5% weight loss was determined from TGA scans performed at 10 °C/min in a N_2 atmosphere. [b]The glass transition temperature (T_g) was determined at the mid point of inflection from DSC scans performed at 10 °C/min in a N_2 atmosphere. [c]T_g was determined from DSC scans performed at 20 °C/min in a N_2 atmosphere.

https://doi.org/10.1021/acs.macromol.1c01998
Macromolecules 2022, 55, 100−112

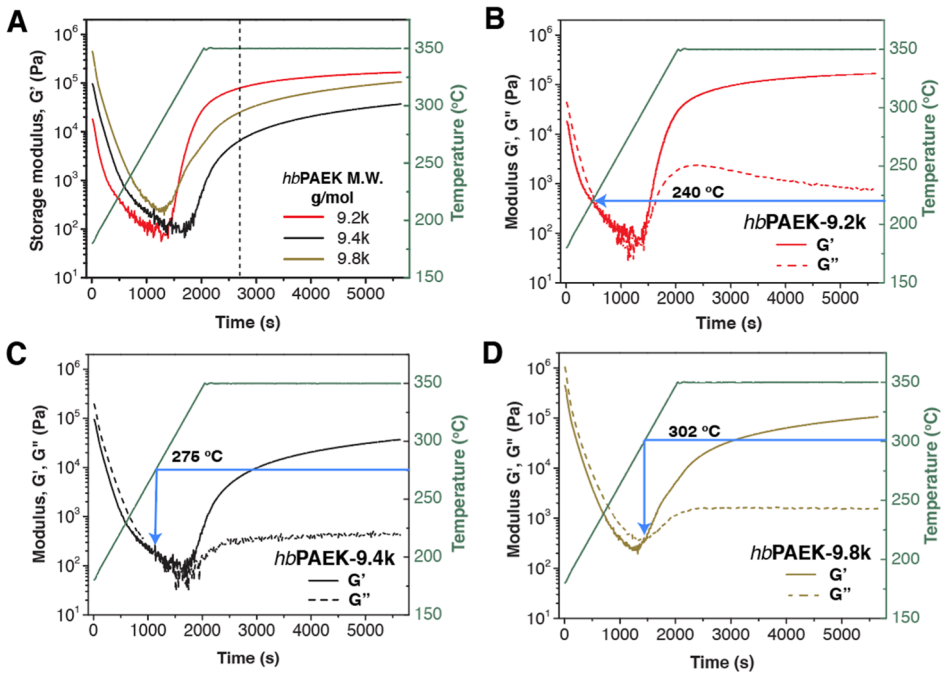

Figure 4. Parallel-plate oscillatory rheology of the *hb*PAEK series. (A) Storage modulus (G') as a function of time from parallel-plate oscillatory rheology (1 Hz, 2% strain, 10 °C/min, with a 1 h isothermal at 350 °C, N_2 atm). For calculations, G' values at the dotted line (t = 2660) are considered. G' and loss modulus (G'') curves as a function of time for (B) *hb*PAEK-9.2k, (C) *hb*PAEK-9.4k, and (D) *hb*PAEK-9.8k. The crossover of G' and G'' is marked with a blue arrow and the corresponding temperature is listed alongside.

3.4. Parallel-Plate Oscillatory Rheology of *hb*PAEKs.

Parallel-plate oscillatory rheology provides more insights into post-condensation and cross-linking chemistries of the *hb*PAEKs in the melt. The storage modulus (G') and loss modulus (G'') curves as a function of time and temperature from isochronal parallel-plate oscillatory rheology (1 Hz, 2% strain, 10 °C/min, N_2 atmosphere) are shown in Figure 4.

The unentangled state of the *hb*PAEK globules was confirmed using stress-relaxation experiments (Figure S6, Supporting Information). For all three *hb*PAEKs, we observe that for the minimum value of stress, the relaxation modulus (G_r) increases with MW and the value of G_r above T_g (≥160 °C) eventually drops by 4 orders of magnitude to values <100 Pa due to its unentangled state. The unentangled state of *hb*PAEK results in amorphous melt flow (see complex viscosity curves in Figure S7, Supporting Information), which in turn results in low values of G', between 100 and 300 Pa (Figure 4). All *hb*PAEKs exhibit a decrease in the G' slope starting at ∼205 °C (Figure 4A). This change in the slope is most pronounced for *hb*PAEK-9.2k, whereas it is barely observable in *hb*PAEK-9.8k. This is presumably caused by an increase in MW resulting from post-condensation reactions between fluoro and remnant phenolate functionalities or between two phenol groups on the *hb*PAEK globular surface. All *hb*PAEKs exhibit a crossover of G' and loss modulus (G'') indicating the gel point due to the formation of a 3D network, that is, cross-linking of globules (Figure 4B−D). The crossover temperature also increases with MW; *hb*PAEK-9.2k = 240 °C, *hb*PAEK-9.4k = 274 °C, and *hb*PAEK-9.8k = 302 °C. With increasing temperature, post-condensation and cross-linking reactions cause G' to increase dramatically (onset at ∼315 °C) and reach values of 10^4−10^5 MPa after a 1 h hold at 350 °C. Additionally, this rate of increase in G' (dG'/dt) decreases with MW, that is, *hb*PAEK-9.2k > *hb*PAEK-9.4k > *hb*PAEK-9.8k.

We summarize the abovementioned results as follows: *hb*PAEKs undergo thermal post-condensation reactions, resulting in an increase in MW (above ∼200 °C), followed by cross-linking at higher temperatures. The multiplicity of hydroxy and fluoro groups on the globular surface, that is, the A_xB_y architecture of the *hb*PAEKs resulting in functionality (f) > 2, facilitates the formation of a 3D network through cross-linking of the globules. Additionally, the trends in crossover time and dG'/dt above 315 °C suggest that the initial *hb*PAEK globular size and the amount of hydroxy groups in the *hb*PAEK are the predominant factors in determining post-condensation and cross-linking reaction rates.

During the isothermal hold at 350 °C, G' plateaus for all *hb*PAEKs and the obtained G' values are dependent on the extent of cross-linking achieved. Using the plateau G' modulus, the effective MW between cross-links (M_c) and the corresponding cross-link density (υ) can be estimated using eqs 5 and 6, respectively.[31,32]

$$G' = \rho RT/M_c \tag{5}$$

where G' is the plateau modulus value after ∼12 min isothermal hold at 350 °C (see the dotted line in Figure 4A), ρ is the density taken from linear PEEK = 1260 kg·m^{-3}, R is the gas constant = 8.314 m^3·Pa K^{-1}·mol^{-1}, and T is the absolute cure temperature = 623.15 K. The cross-linking density (υ) can be calculated using the following equation

$$\upsilon = G'/RT \tag{6}$$

The values of M_c and υ for all polymers are tabulated in Table 4.

From the results listed in Table 4, it is evident that the M_c values obtained for all cross-linked *hb*PAEKs are very high, thereby resulting in small υ values. For comparison purposes, aromatic thermosets prepared from linear phenylethynyl-terminated polyimide oligomers, for example, PETI-SI with

https://doi.org/10.1021/acs.macromol.1c01998
Macromolecules 2022, 55, 100−112

Table 4. Plateau Modulus, Cross-Link Densities, and MW between Cross-Links for the *hb*PAEK Series

*hb*PAEK MW ($g \cdot mol^{-1}$)	G' at 350 °C[a] (Pa)	M_c ($g \cdot mol^{-1}$)	υ (mol m^{-3})
9200	7.6×10^4	8.6×10^4	14.7
9450	6.1×10^3	1.1×10^6	1.2
9800	2.3×10^4	2.8×10^5	4.5

[a]The G' value is obtained after 12 min at 350 °C, see the dotted line in Figure 4A.

an M_n of 9000 $g \cdot mol^{-1}$, exhibit M_c values of ~3619 $g \cdot mol^{-1}$.[33] Aromatic thermosets based on phenol-formaldehyde novolac-cured epoxy resins with precursor M_n values of 800−1400 g/mol exhibit M_c values that are in the range of 120 $g \cdot mol^{-1}$, which is in line with a high degree of cross-linking.[34]

3.5. *hb*PAEK Modified with PEP Cross-Linkable End Groups. Phenylethynyl has been demonstrated to be an efficient chain extender and cross-linker functionality at temperatures above 200 °C (onset of chain extension/cross-linking is a function of concentration and the cross-linker's molecular structure).[35−37] The phenylethynyl functionality was incorporated into our *hb*PAEKs using a phenol derivative, PEP (Scheme 2). We have selected to functionalize *hb*PAEK-9.4k as this polymer is least prone to cross-linking via the existing functionalities (−F, −OH, and −OK) that are present on the *hb* polymer. We prepared three PEP-functionalized *hb*PAEK-9.4k polymers with different molar amounts of PEP, that is, 13, 25, and 35 mol % (Figure S8, Supporting Information). Based on previous work by Frechet's group, we can presume that both linear and terminal fluorine atoms will react equally with a small molecule such as PEP.[38]

Table 5. Thermal Properties of the *hb*PAEK-9.4k−PEP Series

hbPAEK-9.4k−PEP (mol % PEP)	as-prepared		cured *hb*PAEK-9.4k−PEP[a]
	$T_{d,5\%}$[a] (°C)	T_g[c] (°C)	$T_{d,5\%}$[b] (°C)
0	502	151	518
13	524	152	563
25	531	154	542
35	491	132	530

[a]*hb*PAEK−PEP was cross-linked using the cure protocol by heating in a stepwise manner to 350 °C. Details are listed in the Experimental Section and in Section 3.5. [b]The temperature for 5% weight loss was determined from TGA scans performed at 10 °C/min in a N_2 atmosphere. [c]The glass transition (T_g) temperature was determined at the mid point of inflection from DSC scans performed at 10 °C/min.

The thermal properties from TGA and DSC analysis of the synthesized *hb*PAEK-9.4k-PEP series are listed in Table 5 and the TGA and DSC data are shown in Figure S9, Supporting Information. The presence of low-MW impurities results in weight loss at ~300 °C for all synthesized *hb*PAEK-9.4k−PEPs (Figure S9A) and therefore results in lower $T_{d,5\%}$ values (Table 5). Cross-linking of the PEP end groups in the *hb*PAEK-9.4k−PEP series was achieved by heating samples in a stepwise manner under vacuum, 30 °C for 2 h and 45, 60, 100, 200, 300, and 350 °C for 1 h each, followed by slow cooling (overnight) to 30 °C.

In comparison with the as-prepared *hb*PAEK−PEPs, the cured *hb*PAEK-9.4k−PEP powders all exhibit improved thermal stability; no weight loss is observed until 390 °C (Figure S9B, Supporting Information) and $T_{d,5\%}$ occurs at a higher temperature (Table 5). DSC analysis shows that the T_g of the *hb*PAEK-9.4k−PEP series remains largely unchanged upon incorporation of PEP (Table 5 and Figure S9C). The only exception being the 35 mol % PEP sample (entry 4, Table 5) where replacing polar fluoro end groups with apolar PEP end groups results in a reduction in T_g from 151 to 132 °C. Interestingly, the T_g of fully cured *hb*PAEK-9.4k−PEP samples (cured in a stepwise manner to 350 °C) could not be measured by DSC as a flat line devoid of any inflection was obtained.

Parallel-plate oscillatory rheology (20 °C/min, N_2, 2% strain) of the *hb*PAEK-9.4k−PEP series was performed in order to gain insights into cross-linking of PEP functionalities

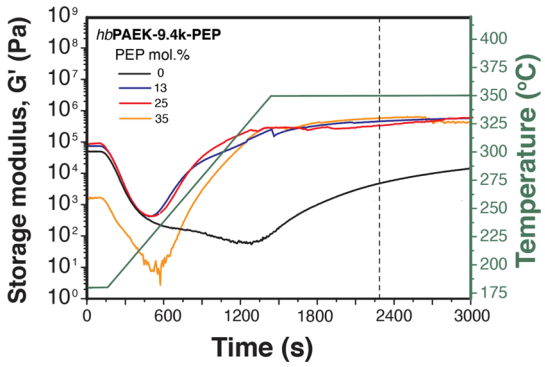

Figure 5. Variation in storage modulus (G') of the *hb*PAEK-9.4k−PEP series heated to 350 °C and held isothermally for 60 min (1 Hz, 2% strain, 10 °C/min). The G' value at the dotted line is considered for calculations of M_c and υ.

Table 6. Plateau Modulus, Cross-Link Densities, and MW between Cross-Links for the *hb*PAEK-9.4k−PEP Series

PEP (mol %)	G' (Pa)[a]	M_c ($g \cdot mol^{-1}$)	υ ($mol \cdot m^{-3}$)
0	6.1×10^3	1.1×10^6	1.2
13	4.4×10^5	1.5×10^4	85.2
25	3.2×10^5	2.0×10^4	62.6
35	5.6×10^5	1.2×10^4	108.5

[a]G' values are taken at t = 2232 s (Figure 5).

in *hb*PAEK-9.4k−PEP (Figure 5). Moreover, rheology facilitates a direct comparison of M_c and υ values between *hb*PAEK with and without PEP (Table 6).

The G' curves overlay until ~235 °C, after which G' for PEP-functionalized *hb*PAEK-9.4k increases rapidly until a plateau modulus of ~10^5 Pa is obtained at ~350 °C (Figure 5). In contrast, G' for neat *hb*PAEK-9.4k without PEP only starts increasing at ~325 °C. Cross-linking of PEP-terminated *hb*PAEK-9.4k seems to be complete, as indicated by a stable G' plateau, when the temperature reaches 350 °C. Neat *hb*PAEK-9.4k does not appear to achieve a stable plateau G' even after ~25 min at 350 °C. In the *hb*PAEK-9.4k−PEP series, cross-linking occurs through both reactions between −F and −OH/−OK functionalities and the reaction of the phenylethynyl-based end groups. In the temperature range of 300−375 °C, phenylethynyl groups react with one another to form both chain extension functionalities (f = 2) and cross-linking functionalities (f = 3 and f = 4) that are typically cyclic in

https://doi.org/10.1021/acs.macromol.1c01998
Macromolecules 2022, 55, 100−112

nature.[39,40] Cross-linking of *hb*PAEK-9.4k−PEP, irrespective of the concentration of PEP used, results in M_c values that are lower by nearly two orders of magnitude than that for neat cross-linked *hb*PAEK-9.4k (Table 6), indicating that PEP is a more efficient cross-link functionality.

3.6. Thermomechanical Analysis of Cross-Linked *hb*PAEK-9.4k−PEP Films by DMTA. The low melt viscosity of the *hb*PAEK-9.4k−PEP series complicates processing using injection molding or compression molding. However, bulk films could be prepared by drying 10 wt % NMP solutions of *hb*PAEK-9.4k−PEP in a vacuum oven, followed by stepwise heating to 350 °C to obtain flexible, robust cross-linked films (Figure 6). In contrast, *hb*PAEK-9.4k without PEP could not be processed into handleable films due to a lack of sufficient cross-links. Only brittle films could be obtained that easily broke into small fragments that could not be used for mechanical testing (Figure 6A).

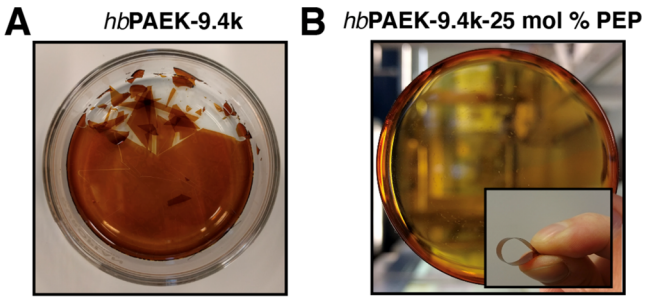

Figure 6. Digital photographs of (A) cross-linked *hb*PAEK-9.4k and (B) free-standing, robust *hb*PAEK-9.4k−25 mol % PEP film. The *inset* in (B) demonstrates the flexibility of the obtained film.

The storage modulus (E') and loss modulus (E'') of the films were determined using DMTA in the tensile mode and the results are shown in Figure 7.

Below T_g, all cured *hb*PAEK-9.4k−PEP films and the *linear* PEKK film exhibit storage modulus values typical of glassy polymers, ∼4 GPa (Figure 7A and Table 7). All films exhibit typical amorphous behavior, that is, their storage modulus drops dramatically when heated past their T_g. From Figure 7B, clear T_g's are observed for all cross-linked *hb*PAEK-9.4k−PEP films that range from 177 to 185 °C. Moreover, T_g for cross-linked 35 mol % *hb*PAEK-9.4k−PEP is 26 °C higher than that of *linear* PEKK. The rubber plateau increases as a function of the PEP concentration, indicating an increase in cross-link density, which is in line with the M_c and υ values, as reported in Table 7.

Table 7. DMTA Results of Cross-Linked *hb*PAEK-9.4k−PEP Thin Films

PEP (mol %)	E' at 30 °C (GPa)	T_g[a] (°C)	E' at 250 °C (Pa)	M_c (g·mol^{-1})	υ (mol m^{-3})
0		films have no mechanical integrity			
13	4.4	177	5.81×10^4	1.0×10^5	11.2
25	3.9	187	1.41×10^5	4.6×10^4	27.2
35	3.8	185	4.10×10^6	1.6×10^3	791.4
linear PEKK	3.7	159	[b]		

[a] T_g is determined from the E'' peak maximum. [b] Film failed at 180 °C.

Above T_g, PEKK becomes too soft for the DMTA measurement to proceed and the measurement was terminated. In contrast, the presence of a cross-linked network in the *hb*PAEK-9.4k−PEP films is manifested in the presence of an E' plateau (Figure 7A). Using E' values at 250 °C, we obtain average M_c values of 1.0×10^5, 4.6×10^4, and 1.6×10^3 g/mol for 13, 25, and 35 mol % PEP, respectively (Table 7). The route used to make free-standing films for this work results in M_c values (Table 7) that are different from those obtained using parallel-plate oscillatory melt rheology (Table 6). More importantly, our results suggest that mechanically stable films using *hb*PAEK-9.4k−PEP can be prepared with M_c values as high as 1.0×10^5 g·mol^{-1}, suggesting that very little cross-linking is needed to prepare free-standing films that are flexible and robust.

At temperatures above 300 °C, the storage modulus (E') increases dramatically for all three *hb*PAEK-9.4k−PEP films (Figure 8A), resulting in E' values up to ∼10 MPa at 400 °C. The increase in E' is most likely the result of an increase in cross-link density. Successive DMTA runs on the same film results in an increase in the plateau modulus (Figure 8A), from 0.14 to 30 MPa, and also in T_g, from 187 to 237 °C (Figure 8B).

3.8. Stress−Strain Measurements. The stress−strain curves for the best cross-linked *hb*PAEK-9.4k−PEP films are summarized in Figure 9. A total of five samples per sample were analyzed, and the average values are listed in Table S1, Supporting Information. A *linear* PEKK film is included for reference purposes.

The Young's moduli for all polymers tested are very similar and fall between 2.0 and 3.0 GPa. The commercial PEKK film

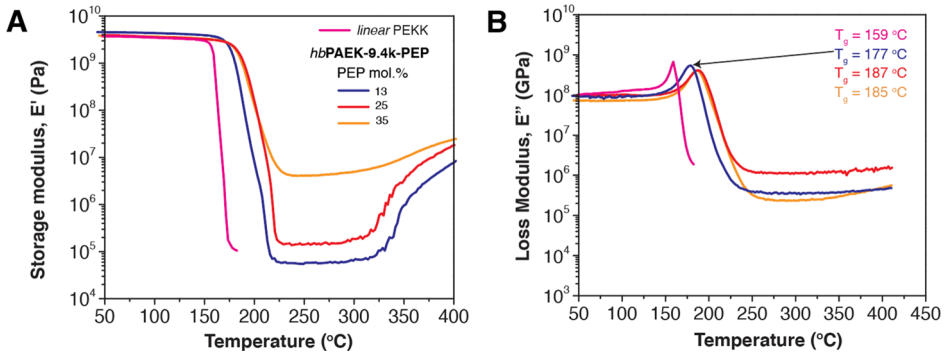

Figure 7. DMTA analysis of cross-linked *hb*PAEK-9.4k−PEP films (2 °C/min heating rate, frequency of 1 Hz, and N_2 atmosphere). (A) he storage modulus (E') and (B) loss modulus (E'') as a function of temperature. The legends for both figures are provided in (A). DMTA curves for a commercially available linear PEKK film is shown for the sake of comparison. T_g is determined from the maximum of the loss modulus peak.

https://doi.org/10.1021/acs.macromol.1c01998
Macromolecules 2022, 55, 100−112

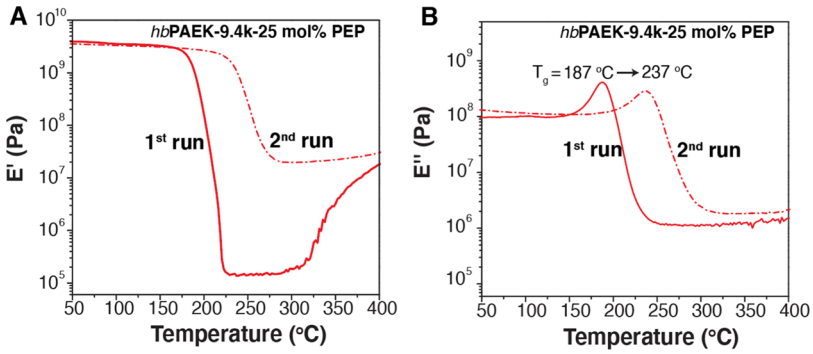

Figure 8. First and second DMTA runs of cross-linked *hb*PAEK-9.4k−25 mol % PEP films. (A) E' and (B) E'' as a function of temperature. Upon termination of the first run at 400 °C, the retrieved film could be measured again to obtain the curve for the second run.

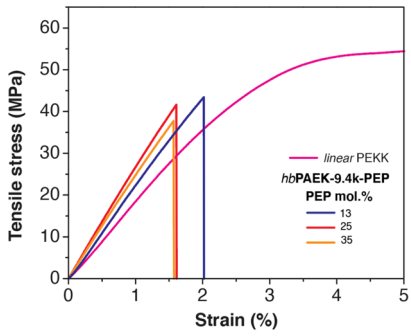

Figure 9. Stress−strain curves collected at 0.1 mm/min of all *hb*PAEK-9.4k−PEP cross-linked films. The tensile properties of *hb*PAEK-9.4k−PEP films are independent of the PEP concentration. A stress−strain curve of a commercial PEKK film is also included for the sake of comparison. The PEKK film strains up to 20% before fracture occurs (not shown here).

exhibits strain-at-break values up to ∼20%, whereas the *hb*PAEK-9.4k−PEP films exhibit maximum strains between 1.5 and 2%. All *hb*PAEK-9.4k−PEP films exhibit ultimate tensile strength values of 40−50 MPa. The toughness of the films can be calculated from the stress−strain curve by integrating the area under the curve. A value of ∼0.3 kJ/m^3 was obtained (Table S1, Supporting Information), which is in the range of typical epoxide-based thermosets.[41] Thus, in terms of stress−strain behavior, the *hb*PAEK−PEP films behave like typical epoxide thermosets as they also exhibit relatively low elongation-at-break values (<5%). A more in-depth study, which is beyond the scope of this work, is required to fully understand how cross-link density, and the nature of the interphase formed, that is, products of cross-linking and chain extension, can be used to tune the mechanical properties of cured *hb*PAEK−PEP films and other (injection) molded articles.

4. CONCLUSIONS

We have demonstrated that *hb*PAEKs can be cross-linked into flexible amorphous films with high T_g's and good mechanical properties. A series of *hb*PAEKs with varying MWs were obtained by polymerizing an AB_2 monomer for 180, 210, and 240 min at 200 °C, respectively. Elemental analysis revealed a mismatch between the actual fluoro groups present and what should be present based on theoretical calculations, and the difference is attributed to the formation of hydroxy groups resulting from hydrolysis of fluoro groups during polymerization. The resulting *hb*PAEKs have an A_xB_y architecture and are polydisperse with DI values of 2.4, 7.3, and 12.5, respectively. The *hb*PAEKs can be post-condensed above 200 °C, where the hydroxy and fluoro groups continue to react and form a cross-linked 3D network. Parallel-plate melt oscillatory rheology experiments show that the MW between cross-links (M_c) ranges from 8.6×10^4 to 2.8×10^5 g·mol^{-1} g·mol^{-1}, which is indicative of a low degree of cross-linking. Cross-linking via this post-condensation route is accompanied by a small increase in T_g from 158 to 169 °C. However, the cross-link density can be increased by incorporating up to 35 mol % phenylethynyl-reactive functionalities. Cure at 350 °C results in a higher cross-linking rate and a higher degree of cross-linking as confirmed by M_c values of 1.6×10^3 g·mol^{-1}. Mechanically robust thin films with a 4 GPa Young's modulus, 44 MPa ultimate tensile strength, and 1.76% elongation at break could be obtained with T_g values as high as 237 °C. All films are amorphous and easy to handle. Our work demonstrates that the network properties of *hb*PAEK films can be controlled by tuning the *hb*PAEK precursor MW, the amount of phenylethynyl end groups, and the cross-linking temperature. The ability to prepare mechanically stable films and tune their network properties can be extended toward other all-aromatic polymer architectures and opens avenues toward structural and functional materials previously not accessible.

■ ASSOCIATED CONTENT

Supporting Information

The Supporting Information is available free of charge at https://pubs.acs.org/doi/10.1021/acs.macromol.1c01998.

^{1}H NMR (600 MHz, $CDCl_3$) of *hb*PAEK, Raman spectra of neat *hb*PAEK-9.4k and the PEP-functionalized *hb*PAEK-9.4k series, AFM measurement process, ^{19}F NMR (600 MHz, $CDCl_3$) of *hb*PAEK, N, D, L, and T calculations for *hb*PAEK, HF gas evolution from mass spectrometry, stress relaxation modulus (G_r) of all *hb*PAEKs as a function of time, complex viscosity of *hb*PAEK when heated to 350 °C, analysis of *hb*PAEK-9.4k−PEP, and TGA, DSC, and stress strain of *hb*PAEK−PEP (PDF)

■ AUTHOR INFORMATION

Corresponding Author

Theo J. Dingemans − *Faculty of Aerospace Engineering, Delft University of Technology, Delft 2629 HS, The Netherlands; Department of Applied Physical Sciences, University of North Carolina at Chapel Hill, Chapel Hill, North Carolina*

27599-3050, United States; orcid.org/0000-0002-8559-2783; Email: tjd@unc.edu

Authors

Wouter Vogel − *Faculty of Aerospace Engineering, Delft University of Technology, Delft 2629 HS, The Netherlands; Dutch Polymer Institute (DPI), Eindhoven 5600 AX, The Netherlands*

Maruti Hegde − *Department of Applied Physical Sciences, University of North Carolina at Chapel Hill, Chapel Hill, North Carolina 27599-3050, United States*

Andrew N. Keith − *Department of Chemistry, University of North Carolina at Chapel Hill, Chapel Hill, North Carolina 27599-3290, United States;* orcid.org/0000-0001-6351-5392

Sergei S. Sheiko − *Department of Chemistry, University of North Carolina at Chapel Hill, Chapel Hill, North Carolina 27599-3290, United States;* orcid.org/0000-0003-3672-1611

Complete contact information is available at: https://pubs.acs.org/10.1021/acs.macromol.1c01998

Author Contributions

W.V. and M.H. contributed equally to this work. The manuscript was written through contributions of all authors. All authors have given approval to the final version of the manuscript.

Funding

DPI Project #718.

Notes

The authors declare no competing financial interest.

■ REFERENCES

(1) Liu, T.; Wang, Y.; Su, Y.; Yu, H.; Zhao, N.; Yang, Y.; Jiang, Z. Preparation and properties of film materials of poly(aryl ether ketone)−based phthalonitrile resins. *Polym. Eng. Sci.* **2015**, *55*, 2313−2321.

(2) Voit, B. I.; Lederer, A. Hyperbranched and Highly Branched Polymer Architectures Synthetic Strategies and Major Characterization Aspects. *Chem. Rev.* **2009**, *109*, 5924−5973.

(3) Voit, B. Hyperbranched Polymers—All Problems Solved after 15 Years of Research? *J. Polym. Sci., Part A: Polym. Chem.* **2005**, *43*, 2679−2699.

(4) Brenner, A. R.; Voit, B. I.; Massa, D. J.; Turner, S. R. Hyperbranched polyesters: End group modification and properties. *Macromol. Symp.* **1996**, *102*, 47−54.

(5) Kwak, S.-Y.; Ahn, D. U. Processability of Hyperbranched Poly(ether ketone)s with Different Degrees of Branching from Viewpoints of Molecular Mobility and Comparison with Their Linear Analogue. *Macromolecules* **2000**, *33*, 7557−7563.

(6) Johansson, M.; Hult, A. Synthesis, Characterization, And UV Curing Of Acrylate Functional Hyperbranched Polyester Resins. *J. Coat. Technol.* **1995**, *67*, 35−39.

(7) Mezzenga, R.; Månson, J. A. E. Thermo-mechanical properties of hyperbranched polymer modified epoxies. *J. Mater. Sci.* **2001**, *36*, 4883−4891.

(8) Hawker, C. J.; Chu, F. Hyperbranched Poly(ether ketones): Manipulation of Structure and Physical Properties. *Macromolecules* **1996**, *29*, 4370−4380.

(9) Baek, J.-B.; Qin, H.; Mather, P. T.; Tan, L.-S. A New Hyperbranched Poly(arylene-ether-ketone-imide): Synthesis, Chain-End Functionalization, and Blending with a Bis (maleimide). *Macromolecules* **2002**, *35*, 4951−4959.

(10) Miao, X.; Meng, Y.; Li, X. Epoxide-terminated hyperbranched polyether sulphone as triple enhancement modifier for DGEBA. *J. Appl. Polym. Sci.* **2015**, *132*, 41910.

(11) Liu, T.; Yan, W.; Su, Y.; Yu, H.; Zhao, N.; Yang, Y.; Jiang, Z. Synthesis and characterization of hyperbranched poly(aryl ether ketone) terminated with phthalonitrile group. *High Perform. Polym.* **2016**, *28*, 263−270.

(12) Kim, Y. H.; Webster, O. W. Hyperbranched Polyphenylenes. *Macromolecules* **1992**, *25*, 5561−5572.

(13) You, K.; Yao, H.; Zhang, Y.; Liu, Y.; Liu, S.; Song, Y.; Guan, S. Phenylethynyl- and naphthylethynyl-terminated hyperbranched polyimides with low melt viscosity. *High Perform. Polym.* **2015**, *27*, 970−978.

(14) Li, X.; Zhang, S.; Wang, H.; Pang, J.; Sun, D.; Mu, J.; Wang, G.; Jiang, Z. Facile synthesis and characterization of hyperbranched poly(aryl ether ketone)s obtained via an A2 + BB′2 approach. *Polym. Int.* **2010**, *59*, 1360−1366.

(15) Mu, J.; Zhang, C.; Wu, W.; Chen, J.; Jiang, Z. Synthesis, Characterization, and Functionalization of Hyperbranched Poly(ether ether ketone)s with Phenoxyphenyl Side Group. *J. Macromol. Sci., Part A: Pure Appl.Chem.* **2008**, *45*, 748−753.

(16) Ghosh, A.; Banerjee, S.; Komber, H.; Lederer, A.; Häussler, L.; Voit, B. Extremely High Molar Mass Hyperbranched Poly(arylene ether)s from a New Semifluorinated AB_2 Monomer by an Unusual AB_2 + A_2 Polymerization Approach. *Macromolecules* **2010**, *43*, 2846−2854.

(17) Yuan, W. Z.; Qin, A.; Lam, J. W. Y.; Sun, J. Z.; Dong, Y.; Häussler, M.; Liu, J.; Xu, H. P.; Zheng, Q.; Tang, B. Z. Disubstituted Polyacetylenes Containing Photopolymerizable Vinyl Groups and Polar Ester Functionality: Polymer Synthesis, Aggregation-Enhanced Emission, and Fluorescent Pattern Formation. *Macromolecules* **2007**, *40*, 3159−3166.

(18) Johnson, R. N.; Farnham, A. G.; Clendinning, R. A.; Hale, W. F.; Merriam, C. N. Poly(ary1 Ethers) by Nucleophilic Aromatic Substitution. I. Synthesis and Properties. *J. Polym. Sci., Part A-1: Polym. Chem.* **1967**, *5*, 2375−2398.

(19) Van BeeK, D.; Fossum, E. Linear Poly(arylene ether)s with Pendant Benzoyl Groups: Geometric Isomers of PEEK or Substituted Poly(phenylene oxide)? *Macromolecules* **2009**, *42*, 4016−4022.

(20) Schneider, S. W.; Lärmer, J.; Henderson, R. M.; Oberleithner, H. Molecular weights of individual proteins correlate with molecular volumes measured by atomic force microscopy. *Pflügers Arch.* **1998**, *435*, 362−367.

(21) Sheiko, S. S.; da Silva, M.; Shirvaniants, D.; LaRue, I.; Prokhorova, S.; Moeller, M.; Beers, K.; Matyjaszewski, K. Measuring Molecular Weight by Atomic Force Microscopy. *J. Am. Chem. Soc.* **2003**, *125*, 6725−6728.

(22) Sheiko, S. S.; Möller, M. Visualization of macromolecules - A first step to manipulation and controlled response. *Chem. Rev.* **2001**, *101*, 4099−4124.

(23) Rivetti, C.; Guthold, M.; Bustamante, C. Scanning Force Microscopy of DNA Deposited Onto Mica: Equilibration Versus Kinetic Trapping Studied by Statistical Polymer Chain Analysis. *J. Mol. Biol.* **1996**, *264*, 919−932.

(24) In, I.; Kim, S. Y. Hyperbranched Poly(arylene ether amide) via Nucleophilic Aromatic Substitution Reaction. *Macromol. Chem. Phys.* **2005**, *206*, 1862−1869.

(25) Flory, P. J. Molecular size distribution in three dimensional polymers I. Gelation. *J. Am. Chem. Soc.* **1941**, *63*, 3083−3090.

(26) Frey, H. Degree of branching in hyperbranched polymers. 2. Enhancement of the DB: scope and limitations. *Acta Polym.* **1997**, *48*, 298−309.

(27) https://www.teinstruments.com/faq/combustion-ion-chromatography (accessed 2021-11-29).

(28) Johnson, R. N.; Farnham, A. G. Poly (aryl Ethers) by Nucleophilic Aromatic Substitution. III. Hydrolytic Side Reactions. *J. Polym. Sci., Part A-1: Polym. Chem.* **1967**, *5*, 2415−2427.

(29) Yang, G.; Jikei, M.; Kakimoto, M.-A. Successful Thermal Self-Polycondensation of AB_2 Monomer to Form Hyperbranched Aromatic Polyamide. *Macromolecules* **1998**, *31*, 5964−5966.
(30) Turner, S. R.; Voit, B. I.; Mourey, T. H. All-aromatic hyperbranched polyesters with phenol and acetate end groups: synthesis and characterization. *Macromolecules* **1993**, *26*, 4617−4623.
(31) Lobo, H.; Bonilla, J. W. *Handbook of Plastics Analysis*; Plastics Engineering, 2003; p 68.
(32) Jiang, H.; Su, W.; Mather, P. T.; Bunning, T. J. Rheology of highly swollen chitosan/polyacrylate hydrogels. *Polymer* **1999**, *40*, 4593−4602.
(33) Gates, T. S.; Whitley, K. S.; Nicholson, L. M.; Hinkley, J. A. How Molecular Structure Affects Mechanical Properties of an Advanced Polymer. *International SAMPE Symposium and Exhibition (Proceedings)*, ISSN 0891-0138, 1999; p 44.
(34) Ogata, M.; Kinjo, N.; Kawata, T. Effects of Crosslinking on Physical Properties of Phenol-Formaldehyde Novolac Cured Epoxy Resins. *J. Appl. Polym. Sci.* **1993**, *48*, 583−601.
(35) Guan, Q.; Norder, B.; Chu, L.; Besseling, N. A. M.; Picken, S. J.; Dingemans, T. J. All-Aromatic $(AB)_n$-Multiblock Copolymers via Simple One-Step Melt Condensation Chemistry. *Macromolecules* **2016**, *49*, 8549−8562.
(36) Guan, Q.; Norder, B.; Dingemans, T. J. Flexible all-aromatic polyesterimide films with high glass transition temperatures. *J. Appl. Polym. Sci.* **2017**, *134*, 44744.
(37) Iqbal, M.; Picken, S. J.; Dingemans, T. J. Synthesis and properties of aligned all-aromatic liquid crystal networks. *High Perform. Polym.* **2014**, *26*, 381−391.
(38) Wooley, K. L.; Hawker, C. J.; Lee, R.; Fréchet, J. M. J. One-step synthesis of hyperbranched polyesters. Molecular weight control and chain end functionalization. *Polym. J.* **1994**, *26*, 187−197.
(39) Hergenrother, P. M. Poly(phenylquinoxalines) Containing Ethynyl Groups. *Macromolecules* **1981**, *14*, 891−897.
(40) Roberts, C. C.; Apple, T. M.; Wnek, G. E. Curing Chemistry of Phenylethynyl-Terminated Imide Oligomers: Synthesis of 13C-Labeled Oligomers and Solid-State NMR Studies. *J. Polym. Sci., Part A: Polym. Chem.* **2000**, *38*, 3486−3497.
(41) Cambridge University Engineering Department. *Materials Data Sources: Materials & Design*, Elsevier, 2003.

https://doi.org/10.1021/acs.macromol.1c01998
Macromolecules 2022, 55, 100−112